

## USE OF VAPORIZING FOIL ACTUATOR FOR IMPACT WELDING OF ALUMINUM ALLOY SHEETS WITH STEEL AND MAGNESIUM ALLOYS

Bert Liu, Anupam Vivek, Glenn S. Daehn

Dept. of Mat. Sc. and Eng., The Ohio State University, 2041 College Road, Columbus, OH 43210, USA, Email: vivek.4@osu.edu

Keywords: Dissimilar joining, vaporizing foil actuator welding, aluminum, steel, magnesium

### Abstract

The vaporizing foil actuator (VFA) is a novel tool for impulse-based metal working operations. In this work, it has been used for impact welding of aluminum flyer sheets to high-strength steel and magnesium plates. Aluminum alloy 6061 sheets of 0.81 mm thickness were launched to velocities in excess of 800 m/s and found to weld to both the target materials investigated: HSLA A588 steel and AM60B magnesium alloy. Grooved as well as flat target plates were utilized. Welding with grooved target plates was found to be not very robust as the weld samples came apart during sectioning. However, the flat targets welded successfully, and during mechanical testing, failure was found to occur outside the joint. The weld interface morphology for each material system and configuration has been shown. Some improvements to the grooved-target experimental configuration are also demonstrated.

### Introduction

Due to the continual push for improving fuel economy and reducing CO<sub>2</sub> emission of vehicles, there is a strong desire to create multi-material lightweight structures [1]. Many parts of the conventional steel car body can be replaced with lighter alloys such as aluminum and magnesium. It then becomes critical to find ways to join these dissimilar metals effectively and reliably. However, most traditional fusion welding techniques are not suitable here, because the high temperatures involved in these joining processes often lead to the formation of brittle intermetallic compounds (IMCs) along the weld interface. On the contrary, solid-state joining techniques, which involves little or no heat input, can be used to produce nearly IMC-free dissimilar joints [2], [3]. Thus, solid-state joining shows much promise for joining dissimilar metals.

In this work, solid-state joining is carried out by vaporizing foil actuator welding (VFAW) [4], which is a impact welding technique, similar to explosion welding, but on a much smaller scale. In impact welding, two metal sheets are brought into a high-speed, oblique impact. Given the right speed and angle, such an impact causes the oxides and other contaminants on the colliding surfaces to be ejected in the form of a jet [5], leaving behind fresh metal surfaces. The fresh surfaces are then immediately brought into intimate contact by the high pressure which ensues from the high-speed impact, thus forming a metallurgical bond [6]. Impact welding does not involve heat input and thus results in little or no heat-affected zones. The low temperature and short time-scale of the welding process also results in little or no interdiffusion and IMC formation.

In VFAW, one member of the colliding tandem is held stationary. The stationary member is called the target. The other member, the flyer, is typically set up parallel to the target, at some stand-off distance away. During the welding event, the flyer is accelerated towards the target and made to collide with it. The driving force

of this acceleration is rapidly expanding plasma derived from the vaporization of a foil actuator. The foil actuator is typically manufactured out of 0.0762 mm-thick low-alloy Al foil, in the shape of a dogbone (Figure 1.(a)), resembling a tensile test sample. The ends of the foil actuator are connected to the output end of a capacitor bank. The capacitor bank is charged to some input energy, typically between 6 and 12 kJ. When the capacitor bank is discharged, a high current rises sharply within the foil and causes it to vaporize into rapidly expanding plasma, which propels the flyer to a high speed (typically 600–1200 m/s) within 10–20  $\mu$ s, over a few millimeters of travel. Previous work [7] has also shown that the temporal evolution of the flyer velocity is very uniform along the active length of the foil actuator. The region of the flyer directly above the foil actuator is expected to be launched flat and that whole section impacts at the measured flyer plate velocity,  $V_p$ . In that region the impact angle,  $\beta$ , is zero, and therefore no welding is observed. However, the rest of the flyer sheet trails behind and folds onto the target as the weld progresses to either side of initial impact region. The experimental assembly and the mechanism of welding process are illustrated in Figure 1.

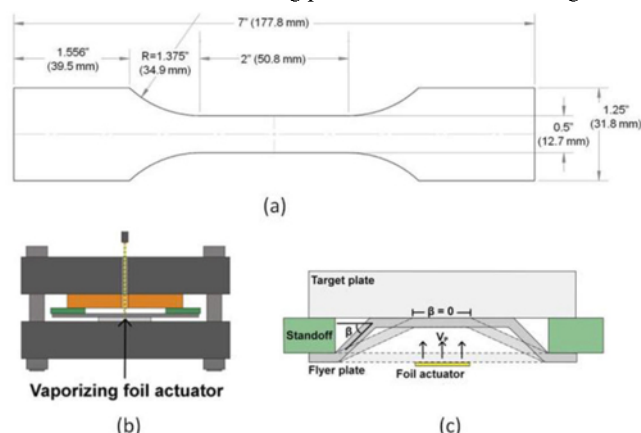


**Figure 1. Schematics of (a) foil actuator, (b) experimental assembly for welding, (c) welding process.**

The VFAW process operates with flyer plates which have thicknesses on the order of millimeters. This process overcomes some of the well-known issues with magnetic pulse welding (MPW), which works on a similar length scale. One of the problems with MPW is longevity of the actuator, which becomes a concern at high driving pressures and low cycle times. The foil actuator, on the other hand, is an easily replaceable, low-cost consumable of every experimental operation, so actuator longevity is not a concern. In addition, the efficiency of the MPW process decreases with the conductivity of the flyer plate material. Conductive driver sheets can be used to launch less conductive materials, but that adds to process time and cost. With the VFAW procedure, the conductivity of the flyer material is immaterial since the pressure is generated from the rapid expansion of the gas and plasma. So far, a variety of dissimilar material combinations,

including Ti-Fe, Fe-Al, Al-Cu, Ti-Cu, Cu-BMG, W-Cu, and Al-Mg, have been welded using this technique [4], [8], [9]. Figure 2 shows the weld interfaces of some of dissimilar material systems which have been welded with.

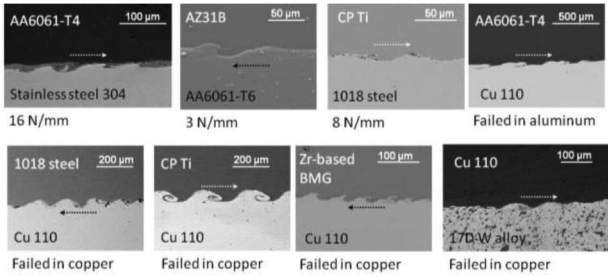


**Figure 2. Welding interfaces of dissimilar joints made by VFAW**

This paper reports on some of the results of research being conducted on the potential use of VFAW for joining automotive alloys of aluminum, iron, and magnesium under U.S. Department of Energy’s Vehicle Technology Program (Grant Number DE-EE006451). Nine dissimilar material pairs involving Fe, Al, and Mg alloys have been attempted for joining in this work, with varying degree of success. Only two pairs will be presented here as representatives: AA6061-T4 to HSLA steel A588 and AA6061-T4 to Mg AM60B. A few discrete welding configurations have been attempted, in search for the most suitable conditions for joining specific material pairs. The results of these experiments will be discussed along with the future outlook for this project. While some mechanical testing has been conducted, this paper focuses on the study of the morphology of the weld interfaces. Impact welds tend to have a wavy interface formed mainly as a result of hydrodynamic flow of the material near the impacted region. Based on the evidence in literature [10]–[12], for material systems that tend to form IMCs, wavy weld interfaces with no or discontinuous IMCs layer are found to be the toughest. Therefore, in this paper, a successful weld would be judged based on the presence of an IMC-free interface, which may be wavy.

### Method

The geometry of the foil actuator used in this experimental campaign and the experimental assembly are shown in Figure 1. The energy source used in these experiments was a Maxwell Magneform capacitor bank with a total capacitance of 426μF, inductance of 100 nH, and short circuit current rise time of 12 μs. When charged to the maximum voltage of 8.6 kV, this capacitor bank can supply 16 kJ of electrical energy. Upon passage of a current pulse, on the order of 100kA, the 0.0762-mm-thick aluminum foil actuator vaporizes and drives the flyer sheet to high velocity. The temporal evolution of the flyer velocity was measured using photonic Doppler velocimetry (PDV) [13]–[15].

Two types of target plates were used: grooved and flat. With flat target plates, the impact angle and velocity change as the flyer sheet collapses onto the target plate. The grooved target plates, where V-shaped grooves of specific pitch angles were machined in, help control the impact angle more precisely [14].

Figure 3 shows the welding setup. The foil actuator was placed on a steel backing block, with polyester layers in between for electrical insulation. The ends of the actuator were connected to the output electrical leads of the capacitor bank. The flyer was

placed against the foil actuator, and the two were electrically insulated from each other by polyester and polyamide layers. Fiberglass composite standoff sheets were used to create the spacing between the flyer and the target. The target, whether flat or grooved, was placed parallel to the flyer, at the standoff distance away. When the grooved target was used, the grooved side faced the flyer. The colliding sides of both the flyer and the target were cleaned by acetone. During the welding event, the foil vaporized and propelled the flyer to collide with the target. Since the flyer was held down on both sides by the standoff sheets, it only bowed up in the center (Figure 1.(c)), along the active area of the foil. The area which corresponds with the center of the foil’s active area experienced a flat impact, whereas the periphery around this active area experienced oblique impact. The area of oblique impact resembled a race track along the periphery of the foil’s active area. Welding was found to occur within this area of oblique impact. On the contrary, when a grooved target was used, since the welding angles were provided by the grooves, welding was found to occur along the center of the foil’s active area, where a flat launch was expected. Welding occurred in the area of oblique impact as well, but only the area of flat launch was interested for analysis when grooved targets were used.

Due to the different types of weld areas when different targets were used, the samples were also sectioned differently. The flat samples were sectioned along the width direction of the foil. This cross section intersects the race-track-shaped weld area at two locations, so usually two distinct weld zones could be found in this type of cross section (Figure 8). The grooved samples were sectioned along the length direction of the foil, along the centerline of the active area. This cross section was believed to have experienced welding angles identical to the predetermined pitch angles of the V-shaped grooves.

Both grooved and flat target plates had dimensions of 50.8 mm x 76.2 mm (W x L). The flyers had dimensions of 101.6” x 76.2”. The flyers were oversized compared to the targets for the sake of mechanical testing which will follow. The material thicknesses depended on the materials available and are summarized in Table 1. In all cases reported in this paper, the flyer material was 0.0762-mm-thick sheet of aluminum alloy 6061 in a T4 temper condition. The grooved target plates were manufactured by electrical discharge machining (EDM). Seven V-shaped grooves were machined side-by-side into each plate (Figure 4). The middle groove was not for analysis but for accommodating the PDV probing hole. The remaining six grooves each had a unique pitch angle, respectively 8°, 12°, 16°, 20°, 24°, and 28°. The standoff distance was typically 1.6 mm, unless otherwise noted. The flyers were launched by the vaporizing foil actuator operating at various input energies, summarized in Table 1. The welded samples were sectioned by abrasive saw for metallography. The flat HSLA steel A588/AA6061-T4 weld sample was also subjected to peel testing in MTS 831.10 load frame moving at a speed of 0.1 mm/sec.

Material	Type	Thickness (inches)	Input energies (kJ)
AA6061-T4	Flyer	0.032	--
HSLA steel A588	Grooved target	0.25	8
HSLA steel A588	Flat target	0.50	9.6 (standoff = 2.4 mm)
Mg AM60B	Grooved target	0.125	4, 6, 7, 8, 10
Mg AM60B	Flat target	0.125	6, 8, 10

**Table 1. Material thicknesses and input energies.**

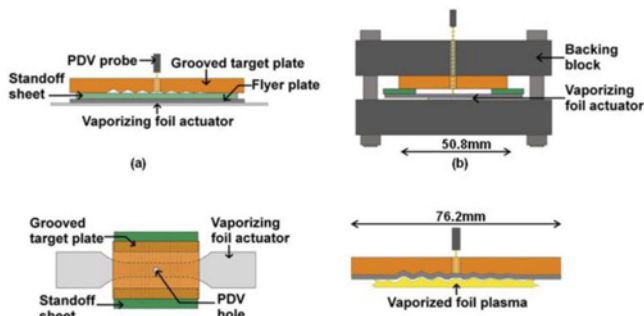


Figure 3. VFAW assembly, (a) side view, (b) front view, including the backing blocks, (c) top view, and (d) side view, during the welding event.

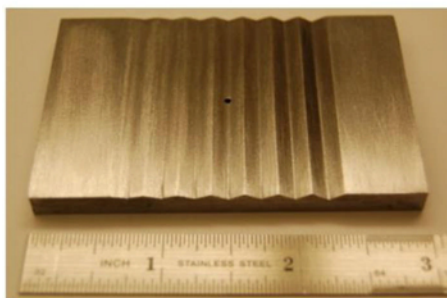
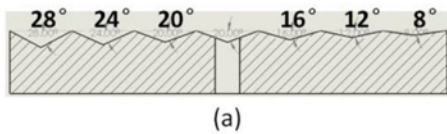


Figure 4. (a) Schematic of grooved portion of the grooved target plate and (b) manufactured grooved target plate.

### Results

The measured flyer velocities at various input energy levels are shown in Figure 5. With increasing input energy, the impact velocity was found to increase. With 1.6mm standoff distance, the estimated plate impact velocity ranged from 488m/s to 822m/s.

#### HSLA steel A588/AA6061-T4

For HSLA steel A588/AA6061-T4 welding experiments, it was observed that the weldment came apart during the experiment itself or during sectioning. The peeled surfaces depicted copious amounts of melting at the interface. Figure 6 shows a typical result from one of these experiments.

However, in the flat configuration, this material system welded successfully and the peel test resulted in failure in the parent aluminum sheet. The peel-tested sample, along with the mechanical test data, is shown in Figure 7. The minimum peel strength for that sample was approximately 40N/mm. The micrograph of the wavy region of the interface also depicts a sharp, high-contrast transition at the weld interface, indicating that IMCs may not have formed. Electro-dispersive spectroscopy (EDS) would be used to verify this.

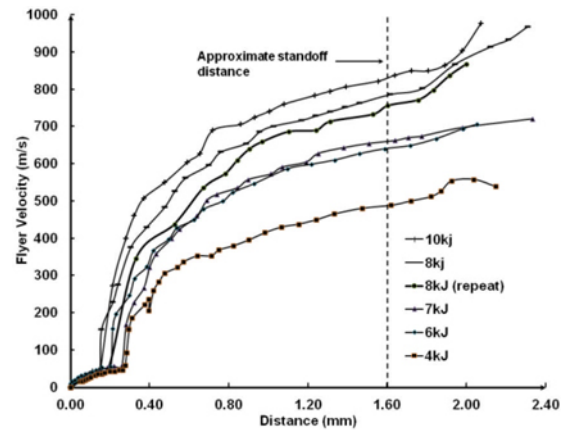


Figure 5. Velocity traces of 0.032''-thick AA6061-T4 flyers at various input energies.

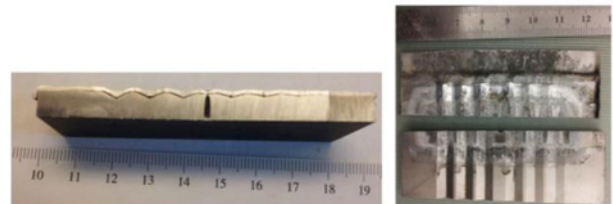


Figure 6. Cross sectional view (left) and peeled surfaces of HSLA 588a/AA6061-T4, with grooved target.

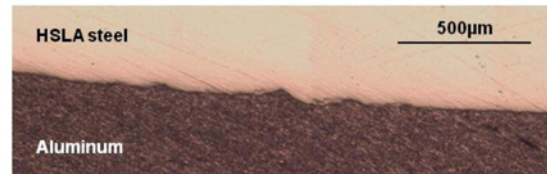
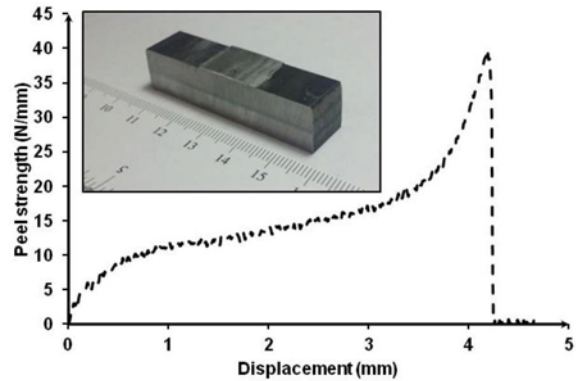
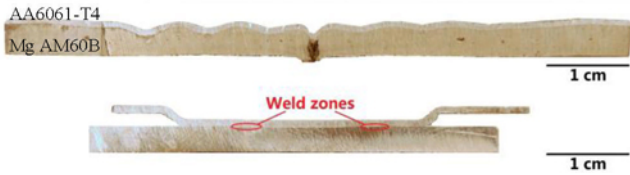


Figure 7. Peel test data (top) and weld interface of HSLA steel A588/AA6061-T4, with flat target

#### AM60B-AA6061

As seen in Figures 8 through 10, this material system was found to weld with both configurations of the target plate. With flat target plates, successful bonding occurred at all energy levels attempted. The interface morphology for each experiment is shown in Figure 10. It can be seen that the amplitude of interfacial

waves increased with higher impact velocities. With grooved target plate, the higher-energy experiments resulted in welding at all angles attempted. At low energies, bonding was seen to occur in some grooves, but those bonds were not robust, since many of them fell apart during sectioning of the samples. The results of the grooved target experiments are shown in Figure 9.



**Figure 8. Cross sections of welded AM60B-AA6061 samples with grooved (top) and flat (bottom) targets.**

Collision velocity, energy Collision angle	488m/s, 4kJ	640 m/s, 6 kJ	660m/s, 7 kJ	787 m/s, 8 kJ	822 m/s, 10 kJ
8°	No weld		1 mm Peeled while cutting		
12°	No weld		Peeled while cutting		
16°	No weld		Peeled while cutting		
20°	No weld	Peeled while cutting			
24°	No weld	Peeled while cutting			
28°	No weld	Peeled while cutting			

**Figure 9. Weld interfaces of AM60B-AA6061 at various impact velocities and angles.**

### Discussion

#### HSLA steel A588/AA6061-T4

Since impact welding involves plastic deformation, stronger materials tend to be more difficult to weld. This can be seen in the case of HSLA steel A588.

It was peculiar that the grooved target did not weld while the flat target did. It was suspected that air and energetic jetted materials may have been trapped in the grooves and caused rebound. These factors are less of a problem with the flat target, since both air and jetted materials could escape through the sides during the welding process. Further developments will follow in a later section.

#### AM60B-AA6061

This material pair welded at a range of speeds and angles. Both wavy and flat interfaces were observed. Wavy interfaces are a typical feature, though not a requirement, for successful welds. However, excessive wavy features, especially ones with vortices, may be an indicator of excessive mechanical energy, which may result in heating, melting, or the formation of IMCs, which hurt the toughness of the joint.

With the grooved targets, higher impact velocities were seen to result in welding over a wider range of angles. For both grooved and flat targets, higher impact velocities also resulted in wavy features with higher amplitudes. The wavy features arise from indenting and shearing actions from the high-speed impact [16], so higher impact velocities tend to result in more pronounced wavy features.

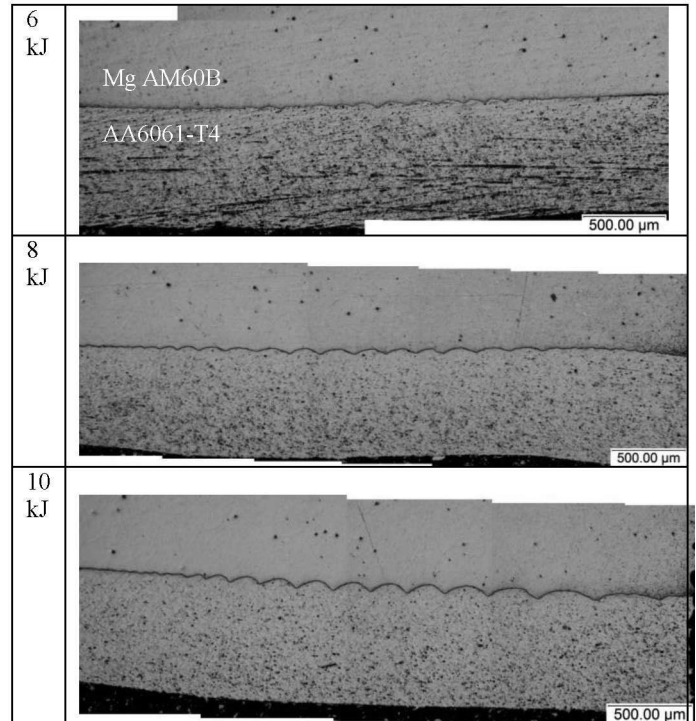


**Figure 10. Weld interfaces of AM60B-AA6061 samples, with flat targets.**

#### Improvements in grooved target experiment

Due to the previous lack of success with Al flyers and HSLA steel grooved targets, the investigation was continued with a similar material pair: AA5052 flyers and HSLA steel A656 targets. In addition, two methods were attempted to aid the welding: vacuum and through slots. Carrying out the welding in vacuum was expected to eliminate the problem of air rebound. The through slots were expected to eliminate the problem of trapped jetted materials by allowing them to escape and leave the weld interface altogether. If there were no through slots, jetted and molten materials were often found accumulating at the bottoms of the grooves.

Both methods were found to improve weldability (Figures 11 and 12). When neither method was used, no welding occurred. When only the vacuum was used, welding only occurred at one of the six angles. When only the through slots were used, welding also only occurred at one angle. However, when both vacuum and through slots were used, welding occurred at all six angles examined. Even when the welding energy was lowered to 8 kJ, with both methods implemented, the pair still welded at five out of the six samples.



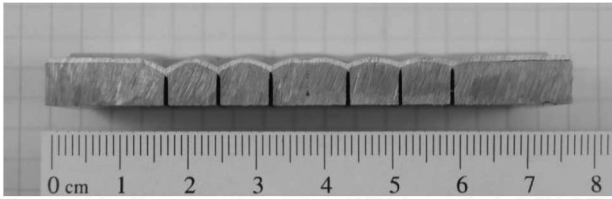


Figure 11. Cross section of a HSLA steel A656/AA5052, welded in vacuum, with through slots, at 10 kJ input energy

In addition, thin interlayers were found to improve welding conditions. Al and Fe interlayers were both attempted, and both were found to help the welding. This is probably due to the distribution of impact energy over the two interfaces, which reduces rebound and the formation of IMCs [17]. Figure 13 shows the result of a 10kJ experiment with AA6061-T4 flyer, 0.25mm thick AISI 1018 steel interlayer, and grooved HSLA steel A656 target. The best bond was found in the 12° groove.

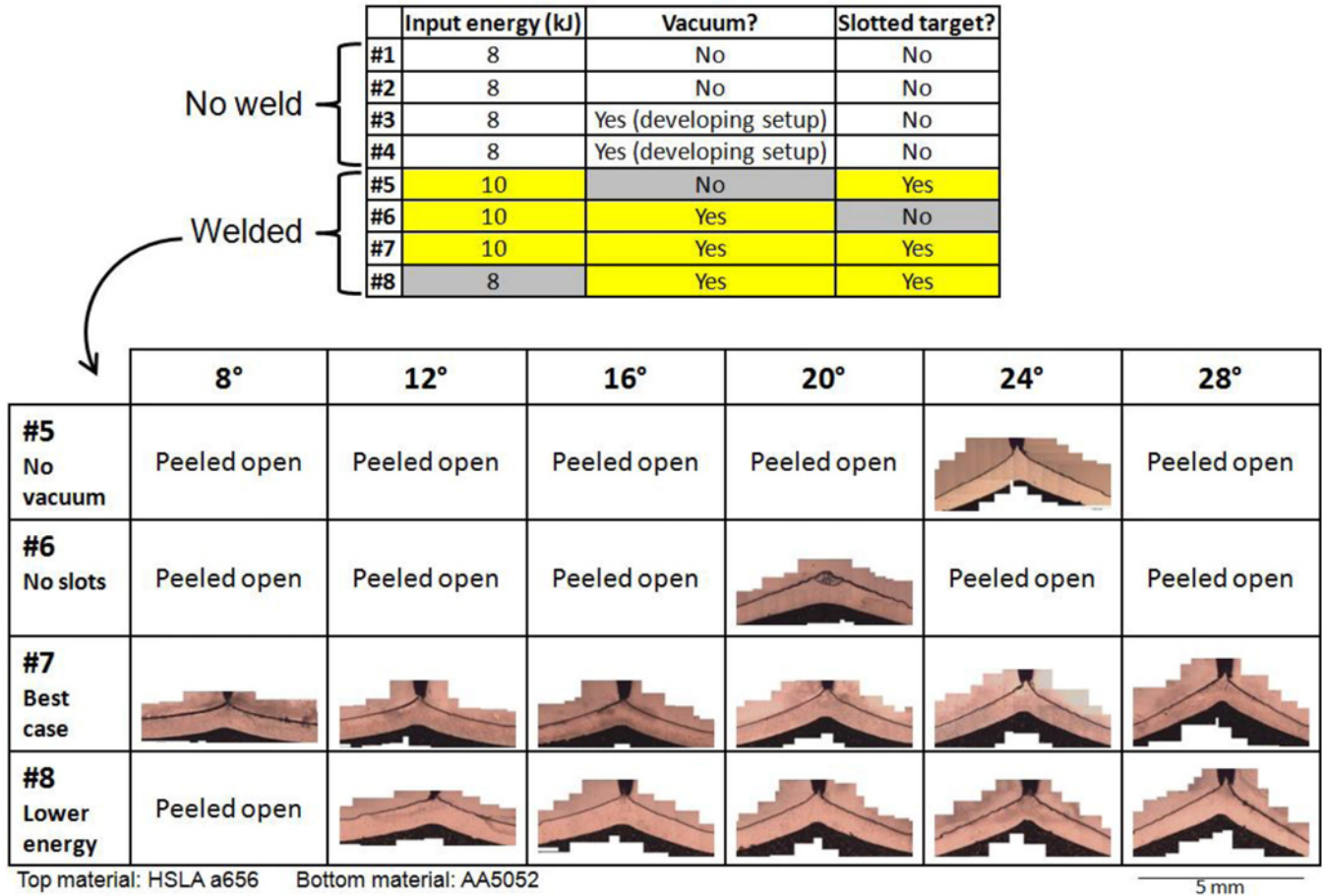


Figure 12. Welding window of HSLA steel A656/AA5052

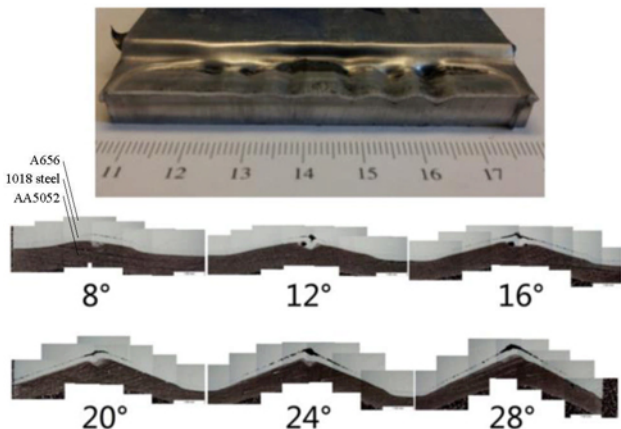


Figure 13. Cross section of HSLA656/1018 steel/AA5052 welded sample.

### Conclusions and future work

Vaporizing foil actuator welding was used in this work to produce solid-state dissimilar joints. Results obtained with two material systems were detailed: HSLA steel A588/AA6061-T4 and Mg AM60B/AA6061-T4. The following conclusions can be made based on this work:

- With input energies as low as 10kJ, 0.81-mm-thick aluminum sheets could be launched to impact velocities in excess of 800m/s within 1.6 mm of travel distance.
- Welding to flat targets is more robust than welding to grooved targets in the case of HSLA steel A588/AA6061-T4. When a flat target was used, this pair welded successfully, and the bond strength exceeded the strength of the AA6061-T4 flyer, whereas

the same material system did not even weld successfully in the grooved target configuration.

- Carrying out grooved-target welding with vacuum, through slots, and interlayers improve welding.
- The amplitude of interfacial waves increases with impact velocity.

Most of the conclusions are based on a qualitative correlation of the measured process parameters and the interface morphology. In order to establish the relationships among process, structure, and property, instrumented mechanical testing on the weld samples would be needed. In related works, it has been seen that even for the samples which fail along the interface, there are some areas where ductile failure occurred within a parent material. This aspect would be investigated further for the relevant material systems through SEM fractography and EDS surface mapping.

Dissimilar joints are particularly susceptible to corrosion. Further investigation will follow to mitigate the problem of corrosion. Methods such as inserting an interlayer with intermediate reduction potential, e-coating, and sealing the joint with a polyurethane sealant would be pursued.

#### Acknowledgement

The authors are grateful for sponsorship from the U.S. Department of Energy's Vehicle Technologies Program (Grant Number DE-EE006451). The views and opinions of authors expressed herein do not necessarily state or reflect those of the U.S. Government or any agency thereof.

#### References

- [1] W. J. Joost, "Reducing Vehicle Weight and Improving U.S. Energy Efficiency Using Integrated Computational Materials Engineering," *Jom*, vol. 64, no. 9, Aug. 2012.
- [2] H. C. Dey, M. Ashfaq, A. K. Bhaduri, and K. P. Rao, "Joining of titanium to 304L stainless steel by friction welding," *J. Mater. Process. Technol.*, vol. 209, no. 18–19, pp. 5862–5870, Sep. 2009.
- [3] O. T. Inal, "Explosive welding of Ti-6Al-4V to mild-steel substrates," *J. Vac. Sci. Technol. A Vacuum, Surfaces, Film.*, vol. 3, no. 6, p. 2605, Nov. 1985.
- [4] A. Vivek, S. R. Hansen, B. C. Liu, and G. S. Daehn, "Vaporizing foil actuator: A tool for collision welding," *J. Mater. Process. Technol.*, vol. 213, no. 12, pp. 2304–2311, Dec. 2013.
- [5] J. M. Walsh, R. G. Shreffler, and F. J. Willig, "Limiting Conditions for Jet Formation in High Velocity Collisions," *J. Appl. Phys.*, vol. 24, no. 3, p. 349, 1953.
- [6] A. A. Akbari Mousavi and S. T. S. Al-Hassani, "Numerical and experimental studies of the mechanism of the wavy interface formations in explosive/impact welding," *J. Mech. Phys. Solids*, vol. 53, no. 11, pp. 2501–2528, Nov. 2005.
- [7] S. Hansen, A. Vivek, and G. Daehn, "Control of Velocity, Driving Pressure, and Planarity During Flyer Launch with Vaporizing Foil Actuator," *Proc. Int. Conf. High Speed Form.*, 2014.
- [8] A. Vivek, B. C. Liu, and G. S. Daehn, "Collision Welding of Tungsten Alloy 17D and Copper Using Vaporizing Foil Actuator Welding," pp. 181–188.
- [9] A. Vivek, S. Hansen, J. Benzing, M. He, and G. Daehn, "Impact Welding of Aluminum to Copper and Stainless Steel by Vaporizing Foil Actuator: Effect of Heat Treatment Cycles on Mechanical Properties and Microstructure," *Metall. Mater. Trans. A*, Jun. 2014.
- [10] A. Durgutlu, H. Okuyucu, and B. Gulenc, "Investigation of effect of the stand-off distance on interface characteristics of explosively welded copper and stainless steel," *Mater. Des.*, vol. 29, no. 7, pp. 1480–1484, Jan. 2008.
- [11] S. A. A. Akbari Mousavi, S. T. S. Al-Hassani, and A. G. Atkins, "Bond strength of explosively welded specimens," *Mater. Des.*, vol. 29, no. 7, pp. 1334–1352, Jan. 2008.
- [12] G. S. Zhang, S. Z. Hou, S. Z. Wei, J. W. Li, and L. J. Xu, "Interface Structure and Properties of Explosive Welded Beryllium Bronze/Steel Composite Plates," *Appl. Mech. Mater.*, vol. 52–54, pp. 1598–1602, Mar. 2011.
- [13] O. T. Strand, D. R. Goosman, C. Martinez, T. L. Whitworth, and W. W. Kuhlrow, "Compact system for high-speed velocimetry using heterodyne techniques," *Rev. Sci. Instrum.*, vol. 77, no. 8, p. 083108, 2006.
- [14] A. Vivek, B. C. Liu, S. R. Hansen, and G. S. Daehn, "Accessing collision welding process window for titanium/copper welds with vaporizing foil actuators and grooved targets," *J. Mater. Process. Technol.*, vol. 214, no. 8, pp. 1583–1589, Aug. 2014.
- [15] J. R. Johnson, G. Taber, A. Vivek, Y. Zhang, S. Golowin, K. Banik, G. K. Fenton, and G. S. Daehn, "Coupling Experiment and Simulation in Electromagnetic Forming Using Photon Doppler Velocimetry," *steel Res. Int.*, vol. 80, no. 5, pp. 359–365, May 2009.
- [16] G. R. Cowan, O. R. Bergmann, and A. H. Holtzman, "Mechanism of bond zone wave formation in explosion-clad metals," *Metall. Mater. Trans. B*, vol. 2, no. November, pp. 3145–3155, 1971.
- [17] P. Manikandan, K. Hokamoto, M. Fujita, K. Raghukandan, and R. Tomoshige, "Control of energetic conditions by employing interlayer of different thickness for explosive welding of titanium/304 stainless steel," *J. Mater. Process. Technol.*, vol. 195, no. 1–3, pp. 232–240, Jan. 2008.